

# NUMERICAL SIMULATIONS OF A FLAT PHANTOM IN THE NEAR-FIELD OF SYMMETRIC DIPOLE ANTENNA

Monika Styła<sup>1,2</sup>, Sebastian Styła<sup>2</sup>

<sup>1</sup>Medical University of Lublin, Faculty of Medicine, Chair and Department of Biophysics, Lublin, Poland, <sup>2</sup>Lublin University of Technology, Faculty of Electrical Engineering and Computer Science, Department of Electrical Engineering and Electrotechnologies, Lublin, Poland

**Abstract.** The paper presents a numerical electromagnetic simulations of SAR limited to human tissues based on FDTD algorithm using Sim4Life platform. Flat-bottomed dielectric vessel (flat phantom) and half-wave symmetric dipole antenna were modeled. Simulations were done for the frequencies 0.9 GHz and 0.6 GHz. The analysis were performed according to the IEEE/IEC62704-1 standard and include distributions of electric and magnetic fields around the phantom and antenna. Finally, SAR distributions in the phantom and near the antenna.

**Keywords:** specific absorption rate, numerical simulation, Sim4Life

## SYMULACJE NUMERYCZNE PŁASKIEGO FANTOMU W BLISKIM POLU SYMETRYCZNEJ ANTENY DIPOŁOWEJ

**Streszczenie.** W pracy przedstawiono numeryczne symulacje elektromagnetyczne SAR dla tkanek ludzkich w oparciu o algorytm FDTD z wykorzystaniem platformy Sim4Life. Zamodelowano płaskodenny dielektryk (fantom płaski) oraz półfalową symetryczną antenę dipolową. Symulacje wykonano dla częstotliwości 0.9 GHz i 0.6 GHz. Analizy zostały wykonane zgodnie ze standardem IEEE/IEC62704-1 i obejmują rozkłady pól elektrycznych i magnetycznych wokół fantomu i anteny. Na koniec zaprezentowano rozkłady SAR w fantomie i poblizu anteny.

**Słowa kluczowe:** współczynnik absorpcji swoistej, symulacje numeryczne, Sim4Life

### Introduction

Starting from the 90s [3, 8, 9, 12, 17] many researchers have made a lot of numerical simulations for the accurate dosimetric evaluation of human tissues models, which are exposed to radiated antennas (e.g. mobile phones) or other wireless communication devices. The electromagnetic interaction between biological tissues and antennas are constantly proven and most of these numerical and experimental results are available in the literature [1, 4–6, 14, 18].

Electric fields are associated with the presence of electric charge but magnetic fields are the result of the physical movement of this electric charge (electric current).

The plane-wave model is a good approximation of the electromagnetic field propagation in the far-field region. In this case, the minima and maxima of magnetic and electric fields arise at the same points along the direction of propagation [7].

In the near-field region the situation is more complicated. The EM field structure might be highly inhomogeneous. In this case, the electric and magnetic fields must be determined.

In addition to the electric and magnetic fields distribution the Specific Absorption Rate (SAR) is one of the most widely used parameters for the evaluation of radiation exposure in the near-field. It is a measure of the rate at which energy is absorbed per unit mass by a human body when exposed to a radio frequency electromagnetic field [19]. It is frequently used to measured power absorbed during magnetic resonance imaging procedures and from mobile phone technologies.

Low SAR can reduces electromagnetic exposure. Now it is possible to modelling SAR distribution by using standardized models of the human body that are filled with liquids that simulate the RF absorption parameters of different human tissues [2, 19].

In this paper we presents simulated SAR distribution in a flat phantom filled with a liquid (HSL, head simulating liquid) with human tissue properties and distribution of electric and magnetic fields around the phantom and dipole antenna.

### 1. Materials and methods

Geometry models, simulations and analysis are made using Sim4Life platform ([www.zmt.swiss](http://www.zmt.swiss)). Sim4Life allows an intuitive approach to the analysis of biomedical phenomena, near-field as well.

The setup of simulation consists of symmetric dipole antenna for tuning over a wide range of frequencies (900 MHz bandwidth in this case), the flat-bottom dielectric phantom, filled with tissue simulating liquid, and the source (a line between dipoles that will be used as a source exciting the antenna). In this case the antenna consist of two conductors (dipoles) of equal length oriented end-to-end with the feedline connected between them [13]. The dipole is the simplest type of the antennas.

#### 1.1. Building a model

The first step of the modelling the setup was creating a geometry of phantom and geometry of dipole antenna (Fig. 1). For simplicity, the phantom was designed as a rectangular box (cube) filled with a mixture with properties such as brain tissue (HLS), described in the next section.

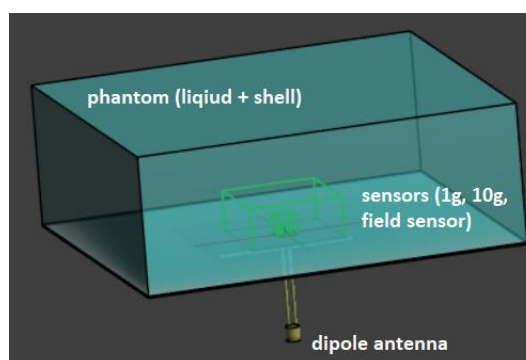


Fig. 1. Symmetric dipole antenna with the phantom (3D view)

Figure 2 illustrates a distance between the shell of the phantom and the antenna. The dipole antenna has been placed under the phantom so that the distance between them could be varied, but the paper presents the only one case that a gap between antenna and phantom is 15 mm. The shell thickness is 2 mm.

Inside the phantom three light green boxes are placed. The biggest box (the field sensor in this case) has dimension 100 mm × 100 mm × 45 mm, in X, Y and Z axis, respectively. The box in the middle is 10g sensor with dimension 21.5 mm in the three planes. The smallest box (1g sensor) has a dimension 10mm in three planes. 1 g and 10 g sensors are required for average SAR distribution pattern.

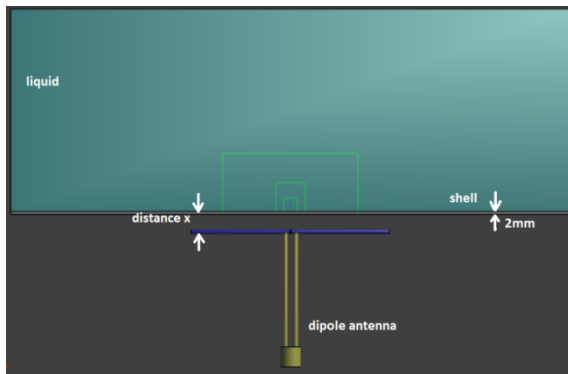


Fig. 2. Schematic diagram showing antenna with the phantom (front view)

## 1.2. Adjusting simulation settings

A methodology of the simulation is to preparing the environment by choosing a type of the simulation and determine properties of the materials. For a near-field issues a FDTD (Finite-difference time-domain method) is recommended. FDTD method uses Maxwell's differential equations to determine electromagnetic field [15, 16]. Additionally, the IEEE/IEC62704-1 standard defines the application of the FDTD technique when used for determining SAR in the human body [7].

PEC is a type of material assigned to all of the parts of dipole antenna. Shell of the phantom has a dielectric properties (relative permittivity  $\epsilon_r$  is 3.1 and mass density is  $1000 \text{ kg/m}^3$ ). The same value of mass density assigned to a tissue-simulation liquid: electrical properties of the liquid: electric conductivity  $\sigma$  is  $0.97 \text{ S/m}$  and relative permittivity  $\epsilon_r$  is 41.5.

Type of signal used to excite a source is Gaussian. Edge source settings were: 0.9 GHz as a center frequency in the first case, amplitude 1 V and resistance  $50 \Omega$ . The second simulation was performed to 0.6 GHz frequency.

Moreover 3 different separated sensors were determined 1 g, 10 g and a field sensor.

A coarse grid with over 824k cells was used in the first simulation. To improve the quality of the simulation results a more precise mesh (fine grid with over 15M cells) was used later. Additionally, Kernel software was used to make a simulation much faster.

## 2. Results

In general, exposure to an electromagnetic field causes in a highly non-uniform deposition and distribution of energy within the body, which must be assessed by dosimetric measurement and calculation.

In the near-field there are strong capacitive and inductive effects from the currents and charges in the antenna. They cause electromagnetic components that do not behave like far-field radiation, therefore it was worth starting with the simulation of the electric and magnetic fields distributions.

### 2.1. Electromagnetic simulations

According to the principle of the interaction of electromagnetic fields with each other, the sources placed inside the object produces a total electromagnetic field simulating the field excited outside the object, whereas the sources placed outside the object produces a total electromagnetic field simulating the field excited inside the object [11].

Figure 3 shows a total near-field distribution of the electric field strength around the antenna for the frequency 0.9 GHz. The maximum electric field strength covers extreme parts of the dipoles and the value is  $5.87 \times 10^{-7} \text{ V/m}$ . Equally large value is located in between two stubs. The electromagnetic field strength decreases with the distance from the antenna and practically do not include the phantom. It can be assumed that increasing the distance between the phantom and the antenna may cause that the electric field inside the phantom will be negligible.

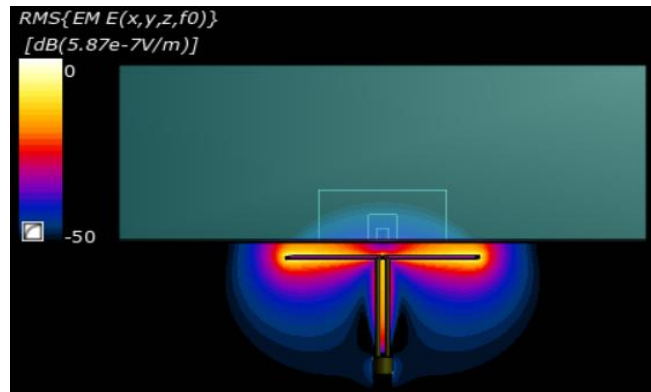


Fig. 3. Distribution of the electric field strength for 0.9 GHz. In the  $xz$  plane. The maximum value is  $5.87 \times 10^{-7} \text{ V/m}$

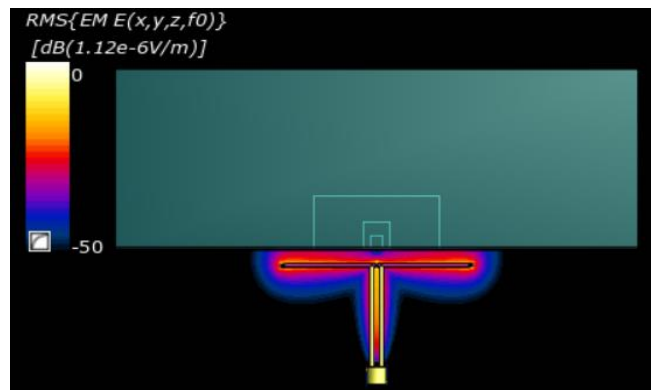


Fig. 4. Distribution of the electric field strength for 0.6 GHz. In the  $xz$  plane. The maximum value is  $1.12 \times 10^{-6} \text{ V/m}$

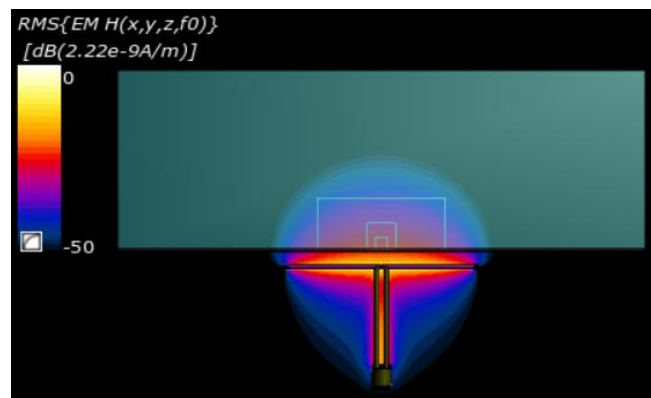


Fig. 5. Distribution of the magnetic field strength for 0.9 GHz in the  $xz$  plane. The maximum value is  $2.22 \times 10^{-9} \text{ A/m}$

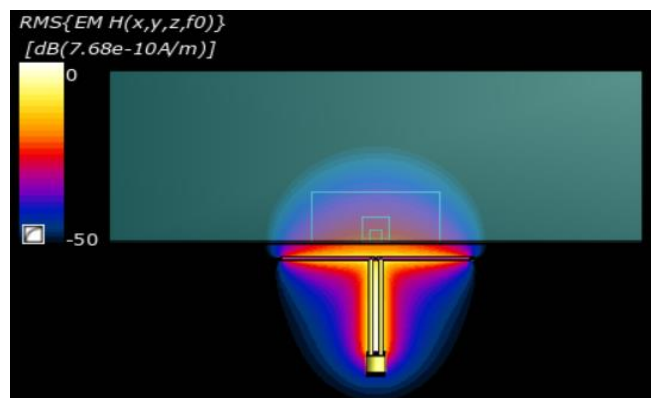


Fig. 6. Distribution of the magnetic field strength for 0.6 GHz in the  $xz$  plane. The maximum value is  $7.68 \times 10^{-10} \text{ A/m}$

In the near-field, both the electric (Fig. 3 and 4) and the magnetic (Fig. 5 and 6) field structures are clearly visible. Interestingly, the electric field strength for the frequency 0.6 GHz does not include the phantom at all. The maximum magnetic field strength for both values of the frequencies places along the whole antenna. Additionally, the spectrum of the magnetic field includes phantoms identically for both frequencies. Figures 5 and 6 show the *xy* planes where the lines of the magnetic field for the frequency 0.9 GHz and 0.6 GHz are centered and arranged circularly.

The input port voltage reflection coefficient is a complex quantity, whose absolute value is an indicator for the reflection.  $|S_{11}| = 0$  means that the circuit is perfectly matched and that none of the incident power wave is reflected [10]. The magnitude of the *S*<sub>11</sub> value is determined by the resistance value (50 Ω) of the antenna.

Reflection coefficient less than -10 dB means the condition where 90% of the signals are successfully transmitted while only 10% is reflected back.

Figure 7 presents the return loss of the dipole antenna and the value is -50dB for the frequency 0.9 GHz. Resonance curve for the frequency 0.6 GHz looks similar and it is negligible in this paper.

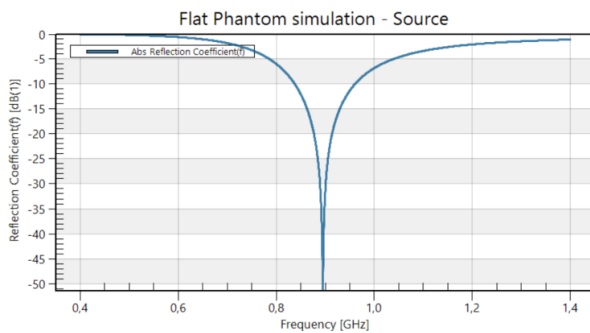


Fig. 7. A plot with the resonance curve of the dipole antenna. The return loss of the dipole antenna in dB

### 2.2. Power balance

Sim4Life platform enables to calculate a power balance value. Ideally, the balance ratio should be 1. The balance ratio is determined as the ratio of total dissipated and input power and for a coarse grid of designed simulation is 0.95. The balance ratio value can be improved by using a better (finer) grid while extending a simulation time. For a fine grid the value is close to 1, as Fig. 8 demonstrated.

Power Balance		
Frequency 9.000e+08 Hz	coarse grid	fine grid
Input Power	3.92465e-21 W	3.9124e-21 W
Lumped Elements Loss	0 W	0 W
Dielectric Loss	3.21236e-21 W	3.36385e-21 W
Radiated Power	5.03578e-22 W	5.18762e-22 W
Balance Ratio (Total Dissipated/Input Power)	0.94682	0.992386

Fig. 8. The result of power balance for coarse grid and fine grid

### 2.3. SAR distributions

For phantom that are equivalent homogeneous tissue, the SAR can be calculated by the formula

$$SAR = \frac{\sigma}{2\rho} E^2 \tag{1}$$

where:  $\sigma$  is the conductivity [S/m],  $\rho$  is the density [kg/m<sup>3</sup>], and  $E$  is electric field [V/m].

Specific absorption rate is usually averaged either over the whole body, or over a small sample volume (typically 1 g or 10 g of tissue). The value of SAR is the maximum level measured in the body part studied over the stated volume or mass. In this paper SAR of the whole phantom was calculated for 0.9 GHz and 0.6 GHz. The results are shown in the figures 9 and 10. The maximum 1 g peak spatial-average SAR is 10.6 W/kg and 9.72 W/kg, respectively.

When measuring the SAR due to a RF exposure, dipole antenna is placed against a representation of a flat phantom. The SAR value is then measured at the place that has the highest absorption rate in the entire phantom, which is usually as close to the dipole antenna as possible.

Figures 9 and 10 illustrate a spatial-averages of SAR for 0.9 GHz and 0.6 GHz, respectively, with moving constant-mass cubes as recommended in IEEE/IEC62704-1 Standard. The SAR is not evenly distributed within the phantom. The maxima of the SAR are clearly concentrated around the central part of the phantom in front of the antenna for both cases. These simulations do not include an area around the antenna.

The maxima SAR values in the *xy* planes for both frequencies are placed in a center bottom surface of the phantom, the nearest surface to the antenna. Figure 11 presents SAR statistics including maximum and minimum SAR position in *xyz*.

According to the IEEE/IEC62704-1 standard [7], the safe SAR limits is 2 W/kg averaged over the 10 g of tissue absorbing the most signal. 3.2 W/kg is the limit of the SAR value for human head tissues.

In case described in this paper, the highest SAR value is in front of the dipole antenna and it greatly exceeds safe limits. Increasing the distance from the antenna may decrease the SAR value.

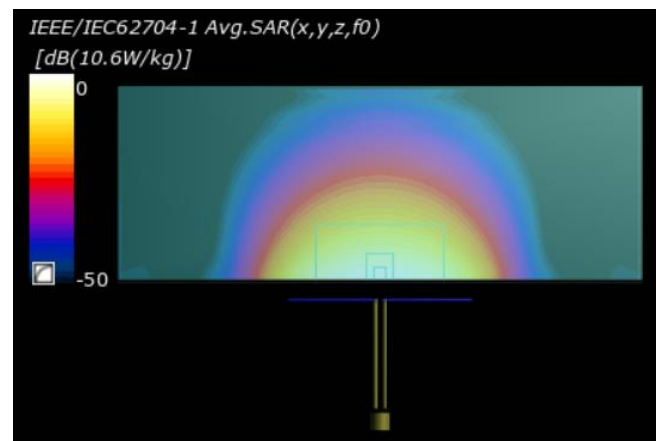


Fig. 9. Peak average SAR for 0.9 GHz in the *xz* plane. The maximum 1 g peak spatial-average SAR is 10.6 W/kg

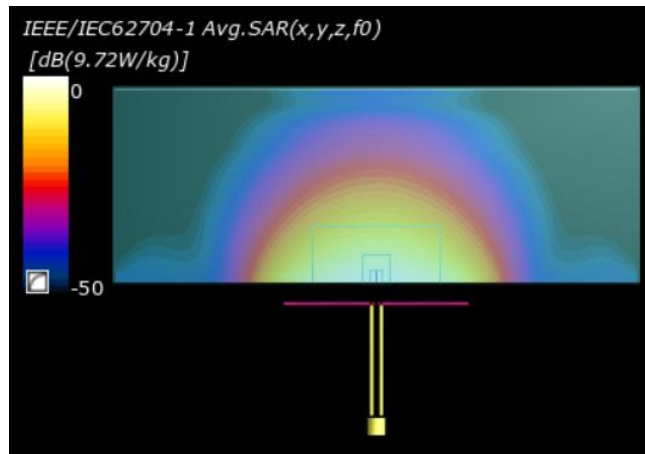


Fig. 10. Peak average SAR for 0.6 GHz in the xz plane. The maximum 1 g peak spatial-average SAR is 9.72 W/kg

SAR Statistics		
	9.000e+08 Hz	6.000e+08 Hz
Min	0 W/kg	0 W/kg
Min Index	(0, 0, 0)	(0, 0, 0)
Min Center	(-0.293213, -0.279713, -0.202351) m	(-0.293213, -0.279713, -0.202351) m
Max	14.8687 W/kg	13.3978 W/kg
Max Index	(57, 48, 38)	(57, 48, 38)
Max Center	(-0.00025, 0.00045, 0.00125) m	(-0.00025, 0.00045, 0.00125) m
Average	0.00523836 W/kg	0.00554689 W/kg
Integral	0.000818508 W/kg	0.000866717 W/kg

Fig. 11. SAR statistics for 0.9 GHz and 0.6 GHz

### 3. Conclusions

The design of a dipole antenna and a flat phantom presented in this paper was performed using the Sim4Life platform with FDTD solver.

The simulations, including return loss of the dipole antenna and specific absorption rate distribution were made for the bandwidth with two different center frequencies. Total near-field distribution of electromagnetic field around the antenna and inside the phantom shows that the electric field is mainly concentrated around the dipoles and the stubs of the antenna, whereas the magnetic field concentrates in the middle of antenna and is arranged circularly. The maximum value of the electric field strength is larger for the lower frequency (0.6 GHz) but the maximum value of the magnetic field strength is larger for the higher frequency (0.9 GHz).

SAR distributions inside the whole phantom were simulated based on recommendation in IEEE/IEC62704-1 standard. The results are specified as maximum 1g SAR and normalized to 1 W radiated power. The maximum SAR values are greatly exceed the permitted limits for the entire sensors placed in the phantom because of a small distance between the antenna and the phantom. The higher value of SAR occurs for the higher frequency of the antenna.

According to the presented results and the remarks discussed above, it can be assumed the local and the average SAR induced due to the radiation from a dipole antenna inside a flat phantom depends on the resonant frequency of the antenna and the distance between the antenna and the phantom. Placing the antenna too close to the phantom causes a very high SAR value.

### References

- [1] Alekseev S. I., Radziewsky A. A., Szabo I., Ziskin M. C.: Local heating of human skin by millimeter waves: Effect of blood flow. *Bioelectromagnetics* 26(6), 2005, 489–501 [http://doi.org/10.1002/bem.20118].
- [2] Andrenko A., Shimizu Y., Wake K.: SAR Measurements of UHF RFID Reader Antenna Operating in Close Proximity to a Flat Phantom. *IEEE International Conference on RFID Technology and Applications (RFID-TA)*, 2019 [http://doi.org/10.1109/RFID-TA.2019.8892054].
- [3] Balzano Q., Garay O., Jr T. J.: Electromagnetic Energy Exposure of the Users of Portable Cellular Telephones. *Vehicular Technology, IEEE Transactions*, 44, 1995, 390–403 [http://doi.org/10.1109/25.406605].
- [4] Bonato M., Dossi L., Gallucci S., Benini M., Tognola G., Parazzini M.: Assessment of Human Exposure Levels Due to Mobile Phone Antennas in 5G Networks. *International Journal of Environmental Research and Public Health* 19(3), 2022, 1546 [http://doi.org/10.3390/ijerph19031546].
- [5] Colombi D., Thors B., Törnevik C., Balzano Q.: RF Energy Absorption by Biological Tissues in Close Proximity to Millimeter-Wave 5G Wireless Equipment. *IEEE Access* 6, 2018, 4974–4981, [http://doi.org/10.1109/ACCESS.2018.2790038].
- [6] Hirata A.: Human exposure to radiofrequency energy above 6 GHz: review of computational dosimetry studies. *Physics in Medicine and Biology* 66, 2021, 08TR01 [http://doi.org/10.1088/1361-6560/abf1b7].
- [7] ICNIRP guidelines for limiting exposure to time-varying electric, magnetic and electromagnetic fields (up to 300 GHz). *Health Physics* 74(4), 1998, 494–522.
- [8] Kuster N., Balzano Q.: Energy absorption mechanism by biological bodies in the near field of dipole antennas above 300 MHz. *Vehicular Technology, IEEE Transactions* 41, 1992, 17–23 [http://doi.org/10.1109/25.120141].
- [9] Kuster N., Kastle R., Schmid T.: Dosimetric Evaluation of Handheld Mobile Communications Equipment with Known Precision. *EICE Transactions on Communications E80-B(5)*, 1997, 645–652.
- [10] Papakanellos P. J., Nanou E. D., Sakka N. I., Tsiafakis V. S. G.: Near field interaction between a brain tissue equivalent phantom and a dipole antenna. *2nd International Workshop on Biological Effects of Electromagnetic Fields*, 2001, 888–897.
- [11] Riu P. J., Foster K.: Heating of tissue by near-field exposure to a dipole: A model analysis. *IEEE transactions on biomedical engineering* 46, 1999, 911–917 [http://doi.org/10.1109/10.775400].
- [12] Schmid T., Egger O., Kuster N.: Automated E-field scanning system for dosimetric assessments. *IEEE Transactions on Microwave Theory and Techniques* 44(1), 1996, 105–113 [http://doi.org/10.1109/22.481392].
- [13] Stutzman W. L., Thiele G. A.: *Antenna Theory and Design*. Wiley, 2012.
- [14] Thors B., Colombi D., Ying Z., Bolin T., Törnevik C.: Exposure to RF EMF From Array Antennas in 5G Mobile Communication Equipment. *IEEE Access* 4, 2016, 7469–7478 [http://doi.org/10.1109/ACCESS.2016.2601145].
- [15] Umashankar K., Taflov A.: A Novel Method to Analyze Electromagnetic Scattering of Complex Objects. *IEEE Transactions on Electromagnetic Compatibility* 4, 1982, 397–405 [http://doi.org/10.1109/TEM.1982.304054].
- [16] Yee K.: Numerical solution of initial boundary value problems involving maxwell's equations in isotropic media. *IEEE Transactions on Antennas and Propagation* 14, 1966, 302–307 [http://doi.org/10.1109/TAP.1966.1138693].
- [17] Yu Q., Gandhi O.P., Aronsson M., Wu D.: An automated SAR measurement system for compliance testing of personal wireless devices. *IEEE Transactions on Electromagnetic Compatibility* 41, 1999, 234 [http://doi.org/10.1109/15.784158].
- [18] Ziskin M., Alekseev S., Foster K., Balzano Q.: Tissue models for RF exposure evaluation at frequencies above 6 GHz. *Bioelectromagnetics – Wiley Online Library* 39, 2018, 17389 [http://doi.org/10.1002/bem.22110].
- [19] [fcc.gov/consumers/guides/specific-absorption-rate-sar-cell-phones-what-it-means-you](http://fcc.gov/consumers/guides/specific-absorption-rate-sar-cell-phones-what-it-means-you) (13.05.2022).

**M.Sc. Eng. Monika Styła**  
e-mail: monika.styla@umlub.pl

Monika Styła graduated from Lublin University of Technology, biomedical engineering. She currently works as assistant in Chair and Department of Biophysics at Medical University of Lublin. Author of 20 scientific papers.

Her research is related to RF coils design and electromagnetic simulations in biomedical applications.

<http://orcid.org/0000-0001-6310-3582>

**D.Sc. Eng. Sebastian Styła**  
e-mail: s.styla@pollub.pl

Sebastian Styła currently works as assistance professor in Department of Electrical Engineering and Electrotechnologies at Lublin University of Technology. He defended his PhD dissertation in Electrical Engineering in 2015. Author of over 50 scientific papers, including 1 patent.

His research is related to the new milling technologies using EM field and diagnostics of electric and electronic automotive equipment.

<http://orcid.org/0000-0002-3239-4433>

